

Fatigue Failure Mechanisms and Fatigue Testing

Thomas Hansson
Volvo Aero Corporation
SWEDEN

1.0 INTRODUCTION

Most failures of engineering components is the result of damage accumulation during cyclic loading at loads well below the ultimate tensile strength of the material used for the component. For these types of failures the term fatigue is used. Fatigue was originally used to describe that the material became tired during applied cyclic loading and lost parts of its virgin strength. Through the use of experimental work, careful microscopy and mathematical modelling work we have increased the understanding of the fatigue phenomena since metal fatigue was first described for steel wires in 1838 [1]. However, surprisingly many issues are not clearly understood and the life predictions of moderately complex components are usually not better than within a factor 2, very often much worse. This implies that further work is necessary to avoid costly failures and unwanted conservatism when designing components subjected to cyclic loading.

2.0 FATIGUE MECHANISMS

Fatigue failure is caused by cyclic loading at loads well below the ultimate tensile strength of materials. In order to cause fatigue damage the material must undergo a permanent change due to the applied cyclic loading. If the applied load is higher than the measured global elastic regime it is easy to observe that the properties of the material have changed. A permanent deformation can be measured and stress and strain can never reach zero at the same time again. This type of fatigue is termed Low Cycle Fatigue or LCF. In most metallic materials the LCF regime in life ranges from a few cycles and up to 10^4 - 10^5 cycles.

If the applied load amplitudes are in the elastic regime it is very difficult to observe any changes in the material on a global level and there is no change in the stress-strain behaviour. However, on a local level small volumes have been subjected to loads exceeding the elastic regime which have caused permanent local damage to the material. This type of fatigue is termed High Cycle Fatigue or HCF. In most metallic materials the HCF regime in life ranges from 10^5 and higher.

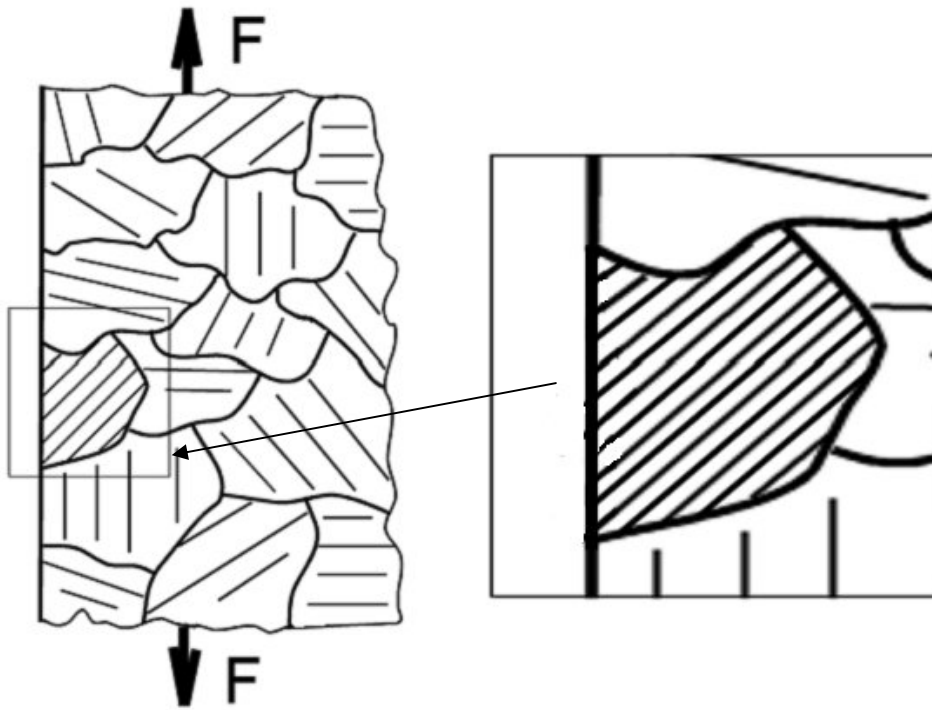
For both LCF and HCF type of loading the fatigue process can be divided in crack initiation and crack propagation. The amount of crack initiation is dependent on the definition of a crack and also if the material is defect free or contain large imperfections.

2.1 Crack Initiation

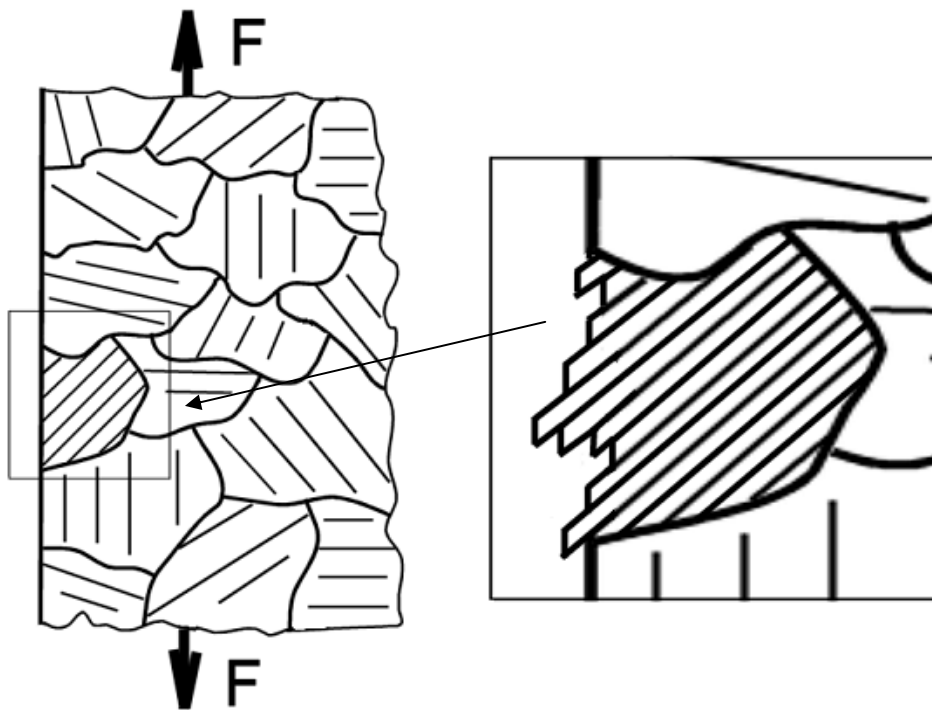
A perfect material does not contain any imperfections such as porosities, inclusions or other defects. However, even a perfect material has a microstructure with characteristic dimensions that in practice will act as imperfections. Of course, no material is perfect but the characteristic dimensions in the microstructure are in many cases a weaker link than the inherent imperfections in the material. In such case the crack initiation can start in a grain with unfavourable direction with respect to the load direction. Each grain is a single crystal which may have very different properties in different directions. In order to initiate a crack, plasticity is needed (even if only locally) and this is, in grain dominated crack initiation, caused by dislocation movement on the slip systems where the required shear stress is at minimum. Plastic deformation by shear is easier at a free surface than in the middle of the material due to constraints from surrounding grains. Consequently crack initiation is nearly always initiated at one of the larger grains at the surface having its favoured slip system in the same direction as the maximum shear direction of the

Fatigue Failure Mechanisms and Fatigue Testing

fatigue load, i.e. 45° inclination to the load direction. The reason why crack initiation predominantly occurs in large grains is that the distance for slip is limited to the size of the grain in the slip direction. Slip in a grain on one slip system will ultimately cause a number of persistent slip bands (see Figures 14-1 and 14-2). These persistent slip bands will move back and forth and finally initiate a crack. The persistent slip bands are difficult to observe except on single crystals where they are allowed to move over very large distances (see Figure 14-2).



(a)



(b)

Figure 14-1: Schematic showing creation of persistent slip-bands during fatigue loading (a) first cycles and (b) close to crack nucleation.

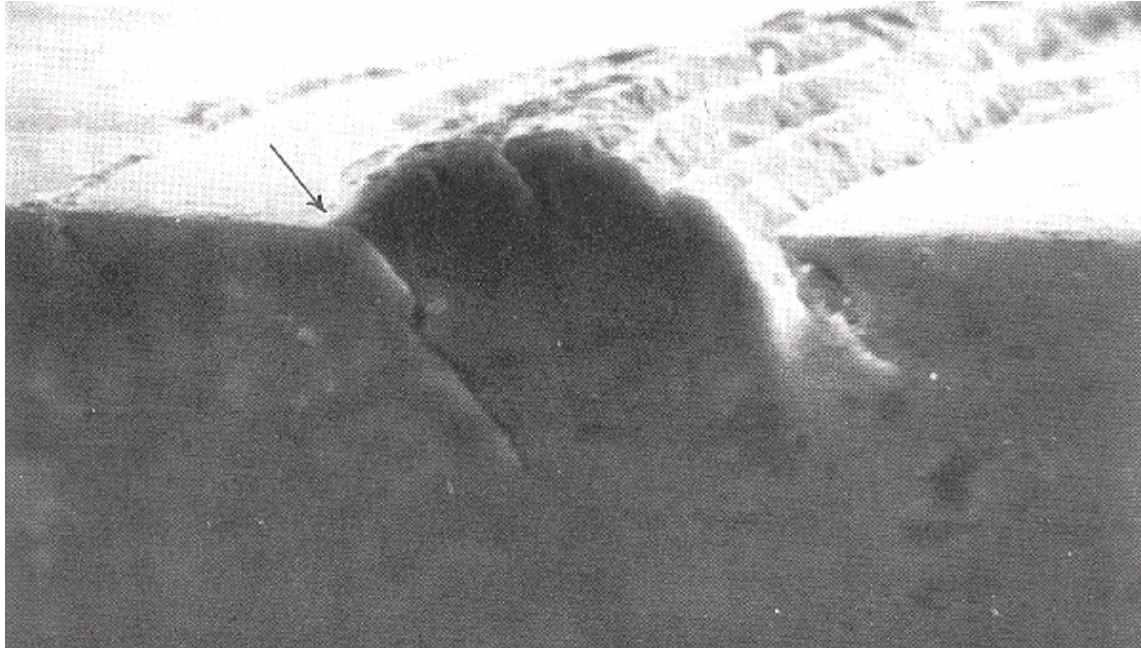


Figure 14-2: Persistent slip bands and a nucleated crack in a Cu-crystal [3].

Some researchers claim that there is no such thing as crack initiation [2]. However, the existence of crack initiation is mainly a question of the definition of a crack. If the minimum size of a crack is of mm size crack initiation exists and may extend over several thousands of fatigue cycles. However, if a crack is defined on an atomic scale the term crack initiation is questionable since crack initiation will occur during the first fatigue cycle or cycles

One possible definition of the end of the crack initiation part could be when the crack changes behaviour from a shear crack to a crack growing perpendicular to the main stress direction (Modus I) (See Figure 14-3).

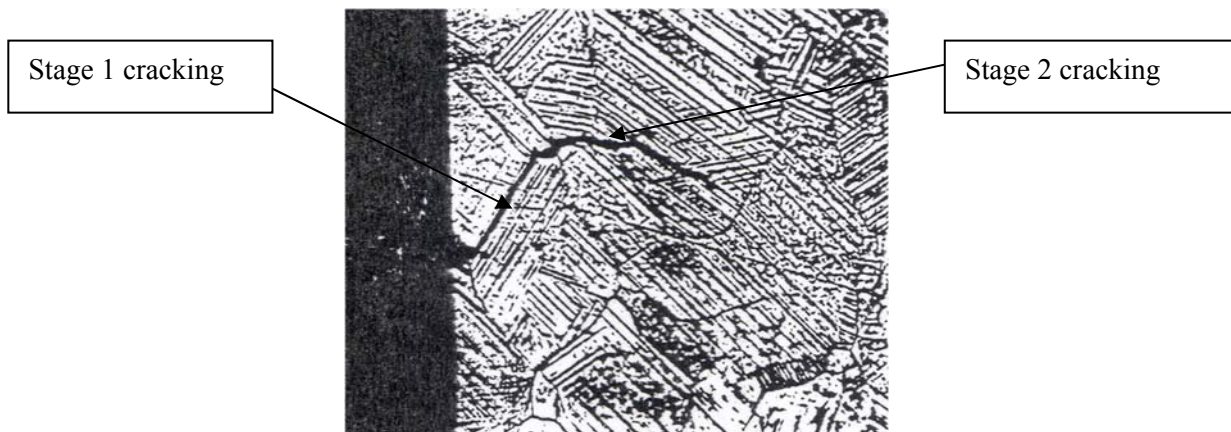


Figure 14-3: Transition from stage 1 to stage 2 (modus 1) cracking.

Crack initiation does not always exist. When the inherent defects in the material or at the material surface are causing the final failure rather than the characteristic dimension in the microstructure the crack initiation part of fatigue can be ignored and the fatigue life is dominated by fatigue crack growth alone.

2.2 Crack Propagation

With the definition of crack initiation made above the crack propagation part of the fatigue life starts when the crack starts to grow perpendicular to the main stress direction. In this case the crack growth can mainly be described as crack growth in modulus 1. Depending on the crack size at the transition from stage 1 to stage 2 the crack may exhibit short crack growth behaviour or not before the growth can be described by linear elastic fracture mechanics (see Chapter 5). The crack growth for short cracks is much faster than that expected from a linear elastic fracture mechanics prediction with data for long cracks. Furthermore, the stage 1 cracking is probably the reason for the short crack growth behaviour. It is not likely that cracks developing at a defect inside the material will exhibit a pronounced short crack growth behaviour, but if they do it is most likely due to absence of crack closure.

3.0 LOW CYCLE FATIGUE

The typical situation for Low Cycle Fatigue in a gas turbine is a temperature driven loading reaching load levels up in the inelastic regime. The start-stop cycles of gas turbines creates large amplitude LCF cycles in many locations in the gas turbine. One of the most common cases is when a local volume reaches a higher temperature than the surrounding environment during start up. In this case the hot area will be subjected to a compressive temperature driven strain that often extend up in the inelastic regime. In fact the described loading cycle is thermomechanical, i.e. both the temperature and strain is varying during the cycle. However, this situation is most often simulated by using materials data from well controlled isothermal strain controlled fatigue tests. For simple loading situations thermomechanical tests may be used to simulate the actual load cases.

Low cycle fatigue testing is usually performed under idealised condition using specimens with well defined surface roughness and restrictions on the allowed residual stresses.

3.1 Low Cycle Fatigue Testing

Low cycle fatigue testing is in most cases carried out in strain control. Depending on the company design system also load controlled tests on specimens with and without notches may be used. At Volvo Aero Corporation primarily smooth specimens tested in strain control are being used. A picture of a typical test set up is presented in Figure 14-4.

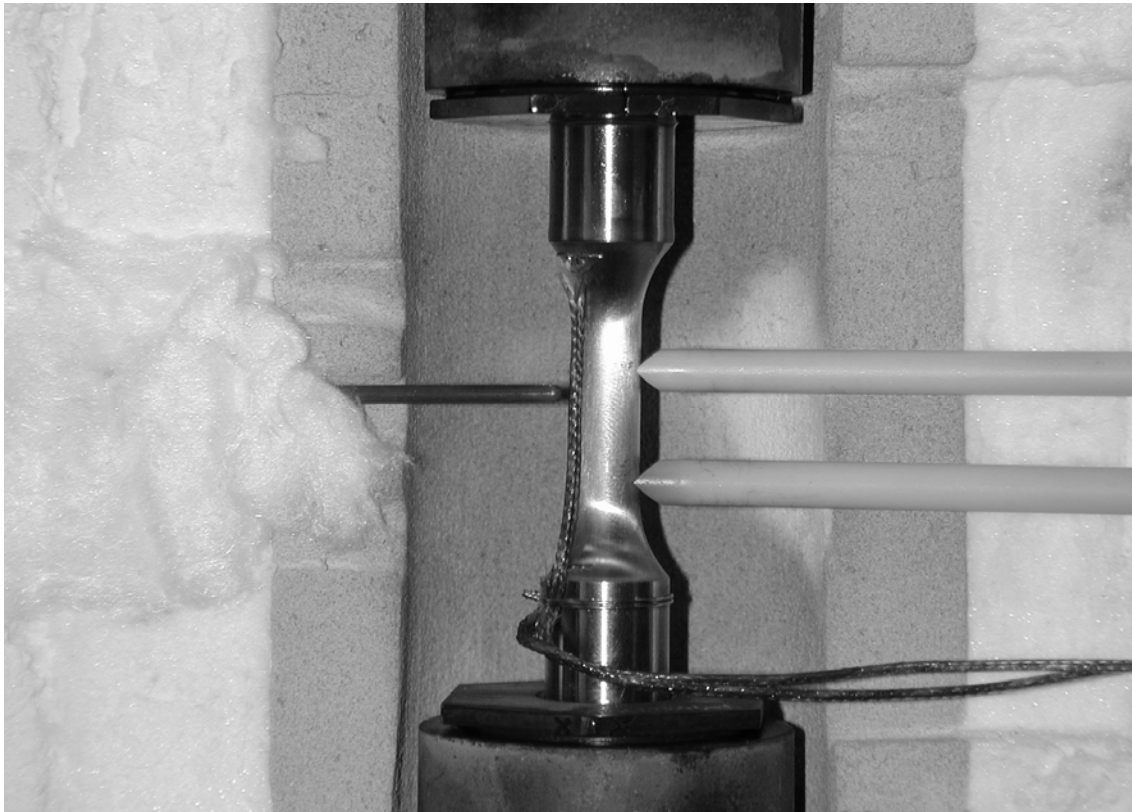


Figure 14-4: Typical set-up for a strain controlled LCF test at elevated temperature.

The important factors in LCF testing are:

- Alignment. During uniaxial testing the alignment is very important. The amount of bending shall be kept as low as possible. In most standards the bending shall be kept below 5% of the average strain at the maximum strain of the lowest strain range used in the test series. The alignment is usually calibrated by using a well machined specimen instrumented with strain gauges at the upper-, mid- and lower part of the gauge section. At each level 3 or 4 strain gauges are equally distributed with 120° or 90° respectively between the strain gauges. The amount of bending is calculated as the difference between the maximum strain and the average strain divided by the average strain. The alignment shall, if necessary, be adjusted so that the bending is minimised. Verification of correct alignment is made by demounting the specimen, turning it in steps of 90°, mounting again and ensure that the amount of bending is below 5% until all the possible positions have been checked. In most cases it is not possible or practical to measure the alignment on every specimen and it is therefore assumed that well machined specimens will be equally well aligned as the calibration specimen. The importance of bending can be easily understood by the following reasoning: 5% bending may result in 5% higher strain range than the measured and this may in turn result in up to about 40% too low measured fatigue life in the low strain range regime. The 40% reduction in life is based on an assumed slope of -0.12 in the lower strain ranges of the $\log N_f - \log \Delta \epsilon$ diagram (see Figure 14-5).
- Strain measurements: In order to avoid buckling of the specimens during the compressive part of the load cycle the gauge section has to be short, usually below 20 mm, and consequently the extensometer measuring strain has a nominal length shorter than the parallel gauge section of the specimen. If the reference length is 12 mm and the strain range to be tested is 1% the difference between the maximum and minimum distance between the measuring points of the extensometer is 0.12 mm. According to most standards the strain range to be tested shall be within 1% (same

reasoning as for the alignment) of the requested strain range which means that the accuracy for measuring the distance between the measuring points has to be 0.0012 mm (or 1.2 microns). Measuring distances between two points at elevated temperature with a precision of 1.2 microns (or sometimes even less) requires high precision extensometers.

- Temperature gradients over the gauge section: If the temperature gradient is not uniform between the points used for measuring the strain the strain is concentrated to the “hot spot” resulting in higher strain than the measured strain and this will give premature fracture in the hot spot and too conservative test results. In most standards the variation in temperature shall be kept within the greater value of $\pm 2^{\circ}\text{C}$ or $\pm 1\%$.
- Measurements of the load: The load is relatively easy to measure and have to be accurately measured within 1% of the measured load.

Ti64 - 300 C - Tangential

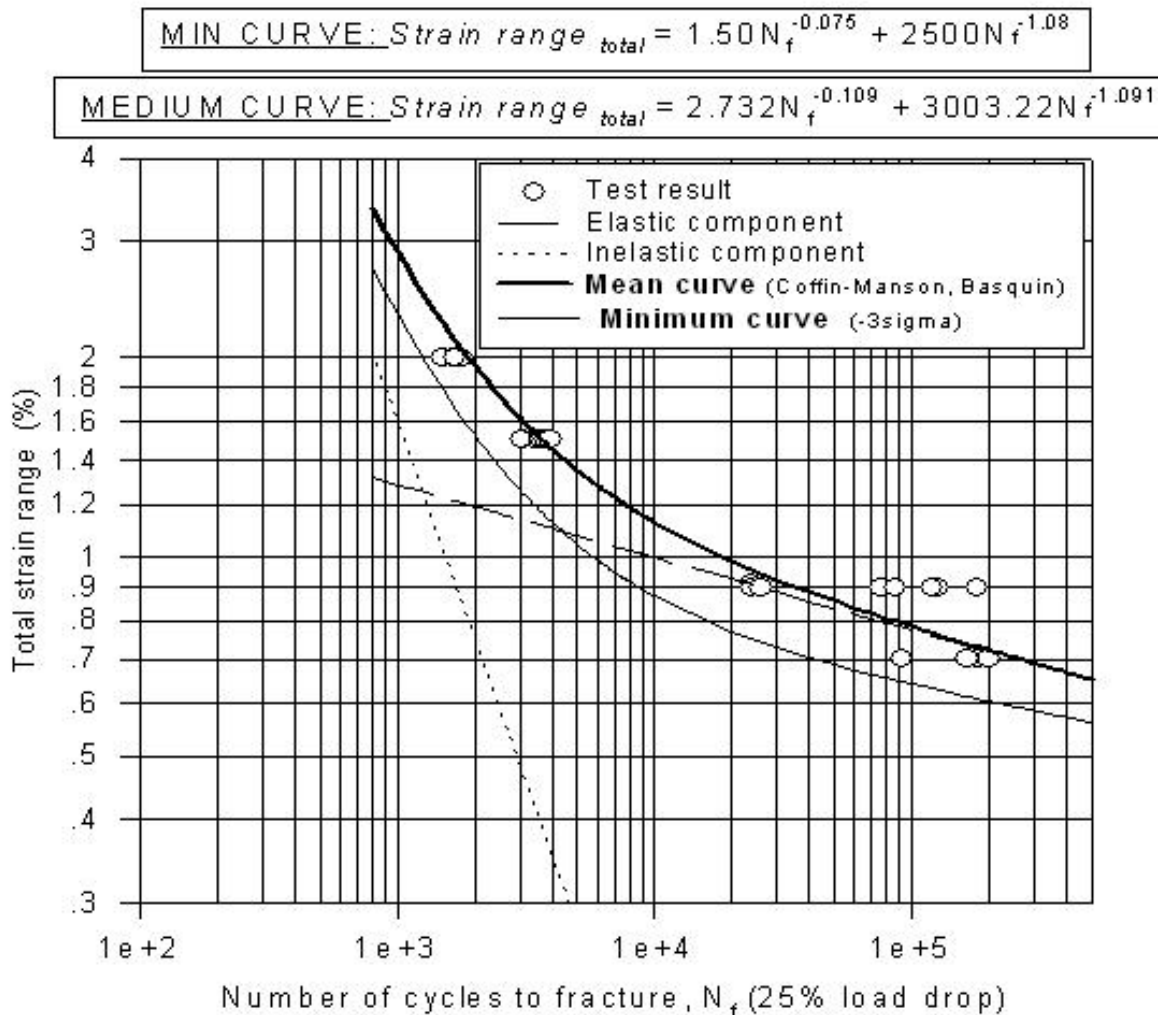


Figure 14-5: Example of fatigue life vs. total strain range for tests evaluated according to the Coffin-Manson, Basquin equation.

3.2 Low Cycle Fatigue – Data Evaluation

Low cycle fatigue data may be evaluated in a number of ways. The most common however, is probably to use the Coffin-Manson, Basquin equation.

Basquin [4] presented an equation for the High cycle fatigue regime that may be expressed as:

$$\Delta\varepsilon_{el} = A \cdot N_f^\alpha \text{ or } \log \Delta\varepsilon_{el} = \log A + \alpha \cdot \log N_f \tag{1}$$

where $\Delta\varepsilon_{el}$ is the elastic strain range, N_f is the number of cycles to failure (or to crack initiation), A is a constant and α is an exponent to be fitted by test data.

Several decades later Coffin and Manson [5,6] independently presented the so-called Coffin-Manson relationship for plastic strains and this equation may be expressed as:

$$\Delta\varepsilon_{inel} = B \cdot N_f^\beta \text{ or } \log \Delta\varepsilon_{inel} = \log B + \beta \cdot \log N_f \tag{2}$$

where $\Delta\varepsilon_{inel}$ is the inelastic strain range, B is a constant and β is an exponent to be fitted by test data.

If we then assume that the total strain range is the sum of the elastic- and plastic strain ranges the Coffin-Manson, Basquin equation may be expressed as.

$$\Delta\varepsilon = \Delta\varepsilon_{el} + \Delta\varepsilon_{inel} = A \cdot N_f^\alpha + B \cdot N_f^\beta \text{ or}$$

$$\log \Delta\varepsilon = \log A + \alpha \cdot \log N_f + \log B + \beta \cdot \log N_f \tag{3}$$

Now if Equations 1 through through 3 are made logarithmic, it is clear that equations 1 and 2 represents straight lines in a $\log\Delta\varepsilon$ - $\log N_f$ diagram. Equation (3) is the sum (in strain) of the two straight lines and at low strain ranges the equation is asymptotically approaching Equation (1) whereas at large strain ranges the equation is asymptotically approaching Equation (2) (see Figure 14-5). This means that both the total strain and the inelastic and elastic strain must be reported together with the number of cycles to crack initiation and/or failure. The type of equations used makes it possible to do a complete separation of the elastic and inelastic stresses and the constants A and B and the exponents α and β may be obtained by fitting the test data to straight lines in a $\log\Delta\varepsilon$ - $\log N_f$ diagram. The exponents α and β represents the slopes of equations (1) and (2) respectively while the strain values at $N_f = 1$ represents $\log A$ and $\log B$ of the equations (1) and (2) respectively. It is to be noted that the curve fit shall be made using $\log N_f$ as the independent variable which requires rearrangement of Equations 1 and 2.

Another curve obtained from low cycle fatigue testing is the cyclic stress-strain curve. The cyclic stress-strain curve is for example used for calculating the applied strain range for a certain elastically calculated load range. Alternatively the stresses and strains are calculated using an elasto plastic FE- analysis with the cyclic stress-strain curve as input to the calculation. The cyclic stress strain curve is usually measured at the mid-life cycle hysteresis loop or the hysteresis loop recorded nearest to the real mid-life cycle. The values taken from the mid-life hysteresis loop are: stress range ($\Delta\sigma$), total strain range ($\Delta\varepsilon$), elastic strain range ($\sigma\varepsilon_{el}$), inelastic strain range ($\Delta\varepsilon_{inel}$) and mean stress (σ_{mean}) if applicable (see Figure 14-6). The cyclic stress-strain curve is often expressed using a Ramberg-Osgood type of relationship:

$$\frac{\Delta\varepsilon}{2} = \frac{\Delta\sigma}{2E} + \left(\frac{\Delta\sigma}{2K'} \right)^{\frac{1}{n}} \tag{4}$$

E is the Young's modulus and the constant K and the exponent (1/n) can be obtained considering only the inelastic strain range:

$$\frac{\Delta \varepsilon_{inel}}{2} = \left(\frac{\Delta \sigma}{2K} \right)^{\frac{1}{n}} \text{ or } \log \left(\frac{\Delta \sigma}{2} \right) = \log K + n \cdot \log \left(\frac{\Delta \varepsilon_{in}}{2} \right) \quad (5)$$

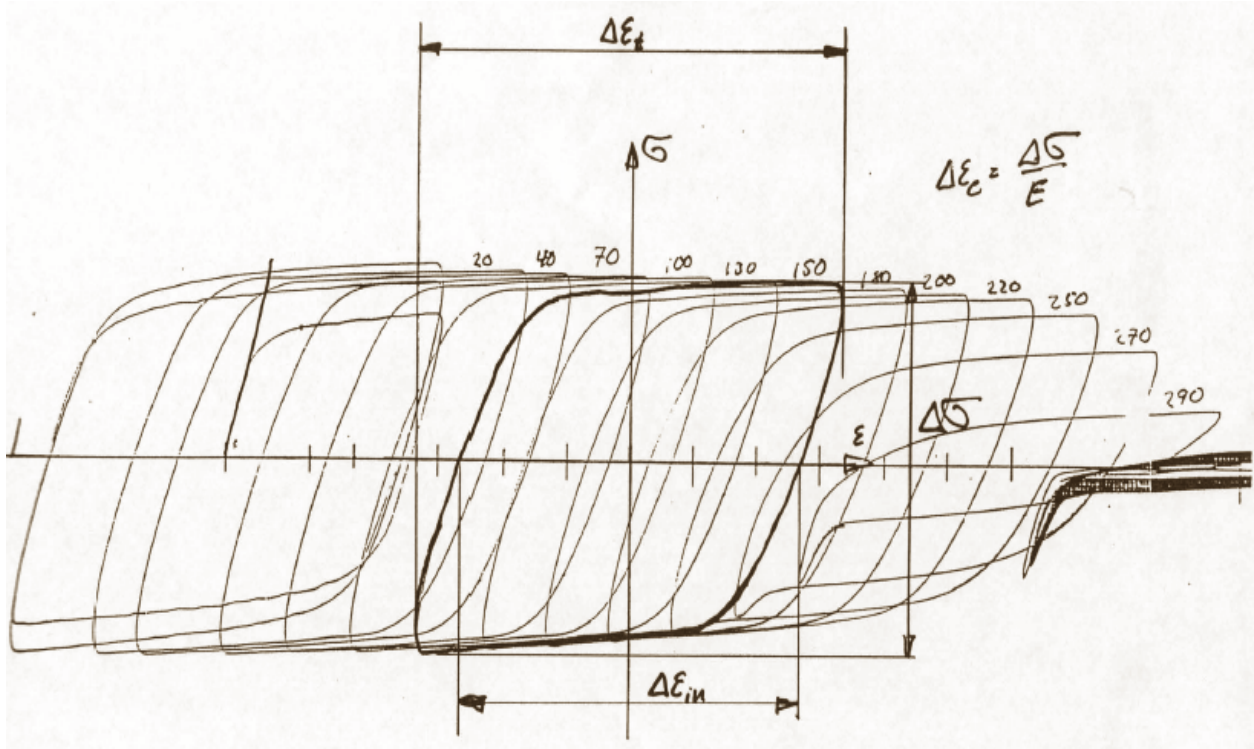


Figure 14-6: Example of hysteresis loops obtained from a strain controlled LCF tests at a high strain range. The highlighted hysteresis loop is the one closes to the mid-life cycle.

The exponent n or (1/n) and the constant K are calculated by fitting the obtained $\log(\Delta\sigma/2)$ and $\log(\Delta\varepsilon_{inel})$ to equation (5).

Figure 14-7 is an example of a cyclic stress-strain curve for a cast Ni-base superalloy. The scatter in stress is usually much higher for cast materials than for forgings or sheet material.

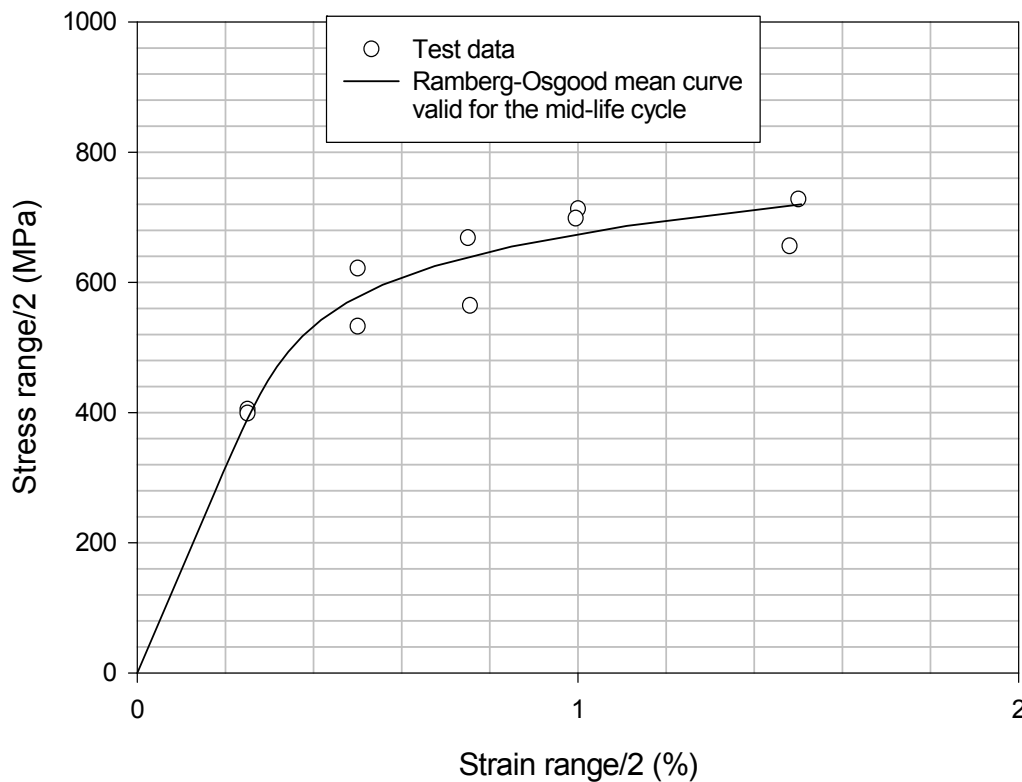


Figure 14-7: Cyclic stress-strain curve for a Ni-base superalloy at 1000K.

3.3 Statistical Aspects

Often for detailed design, minimum fatigue data has to be used when estimating the fatigue life of components. In most cases the requirement is to use minimum data with 95% confidence that 99% of the test results have longer life than the value provided (often called 95/99 curve).

There are a number of ways to do this, but one way is to use the so-called k-Sigma concept [7]. First it has to be assumed that results for $\log N_f$ can be described by a normal distribution. Also it has to be assumed that the standard deviation in $\log N_f$ is constant for all results in the elastic and inelastic regime respectively. The equations (1) and (2) can now be treated separately:

$$\log N_f^{\min} = \log N_f^{\text{mean}} - k_{el} \cdot s_{el} \tag{6}$$

and

$$\log N_f^{\min} = \log N_f^{\text{mean}} - k_{inel} \cdot s_{inel} \tag{7}$$

where

N_f^{\min} is the minimum life, N_f^{mean} is the mean life calculated from Equation 3, k_{el} and k_{inel} are the k-factors to be used for the elastic and inelastic data respectively and s_{el} and s_{inel} are the calculated standard deviations in life calculated using Equation (8).

$$s = \sqrt{\frac{\sum_{i=1}^n (\log N_{f,i}^{measured} - \log N_{f,i}^{mean})}{n - 2}} \tag{8}$$

The factors k_{el} and k_{inel} depend on the number of test data used for the evaluation. In the normal case more data points are available for the elastic strain ranges than for the inelastic strain ranges since for tests at small strain ranges the inelastic strain range equals zero. Table 14-1 provides k to be used for different number of values used to calculate the standard deviation. If the number of results used for calculating the standard deviation are larger than 25 the 95/99 curve approaches the -3 Sigma curve. The used methodology may be used to calculate other type of minimum curves such as the 90/95 (90% confidence that 95% of the tests have longer life than the curve).

Table 14-1: Table showing the k to be used for different number of results used for the analysis.

| Number of results in the analysis | 90/95 | 95/99 |
|-----------------------------------|-------|--------|
| 3 | 5.310 | 10.552 |
| 4 | 3.957 | 7.072 |
| 5 | 3.400 | 5.741 |
| 6 | 3.091 | 5.062 |
| 7 | 2.894 | 4.641 |
| 8 | 2.755 | 4.353 |
| 9 | 2.649 | 4.143 |
| 10 | 2.568 | 3.981 |
| 11 | 2.503 | 3.852 |
| 12 | 2.448 | 3.747 |
| 13 | 2.403 | 3.659 |
| 14 | 2.363 | 3.585 |
| 15 | 2.329 | 3.520 |
| 16 | 2.299 | 3.463 |
| 17 | 2.272 | 3.415 |
| 18 | 2.249 | 3.370 |
| 19 | 2.228 | 3.331 |
| 20 | 2.208 | 3.295 |
| 21 | 2.190 | 3.262 |
| 22 | 2.174 | 3.233 |
| 23 | 2.159 | 3.206 |
| 24 | 2.145 | 3.181 |
| 25 | 2.132 | 3.158 |

Sometimes there is a need to present mean data in terms of 95/50 data rather than the 50/50 data that is usually obtained from the data evaluation. Figure 14-8 shows the difference between two different mean curves, the 50/50 curve and the 95/50 curves. There is a small but clear difference between the two curves, but we have to keep in mind that the tests were conducted on a cast material showing a significant amount of material scatter.

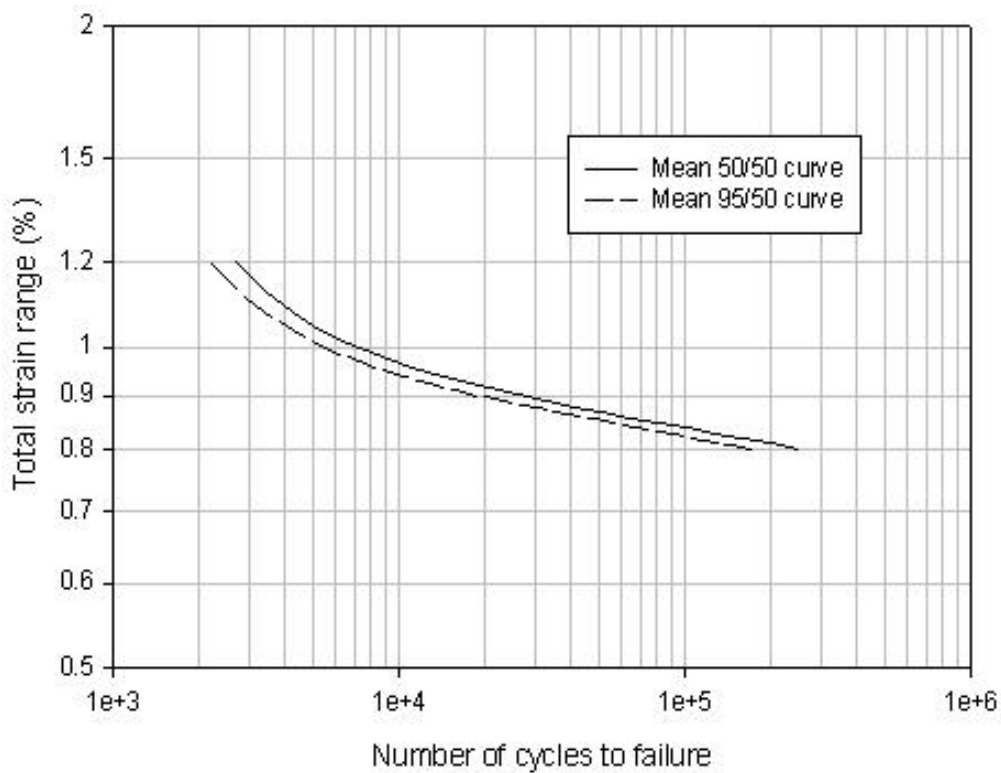


Figure 14-8: LCF curves showing mean data with 50% (50/50) and 95% (95/50) confidence levels.

3.4 Mean Stress Effects

It is quite clear that the R-ratio ($\epsilon_{min}/\epsilon_{max}$) plays an important role for the LCF life, especially at low strain ranges. At high strain ranges the mean stress will tend to move towards zero.

There are a number of ways to compensate for a different R-ratio and the most common approaches are:

Morrow:

$$\Delta\epsilon = \left(A - \frac{2 \cdot \sigma_{mean}}{E} \right) \cdot N_f^\alpha + B \cdot N_f^\beta \quad (9)$$

which is a mean stress correction of the Basquin Equation.

Smith-Watson-Topper:

$$P_{SWT} = \sqrt{\frac{\sigma_{max} \cdot \Delta\epsilon \cdot E}{2}} \quad (10)$$

And this expression is calculated for all $\Delta\epsilon$ and N

Walker:

$$\Delta\epsilon_{R=0} = \Delta\epsilon_{R \neq 0} \cdot (1 - R)^{m-1} \quad (11)$$

where m is fit to experimental data.

4.0 HIGH CYCLE FATIGUE

The typical situation for a high cycle fatigue (HCF) problem in a gas turbine is vibrations of relatively low amplitude and high frequency. The HCF Vibrations are usually purely linear elastic even if the mean stress (or strain) may be up in the inelastic regime for the first load cycle or cycles. However, even if no inelastic strains can be measured globally local volumes will experience inelastic strains otherwise failure will never occur and we are below the fatigue limit of the material.

The fatigue limit, $\Delta\sigma_n$, is in most cases defined as the fatigue stress range when specimens survive 10^7 cycles. The choice of 10^7 cycles is made due to practical reasons. In a servo-hydraulic test machine with a maximum frequency of 30-50 Hz it takes between 2 and 4 days to complete a test lasting for 10^7 cycles. Using a fatigue limit of 10^8 or 10^9 cycles would require test times of 20-40 and 200-400 days respectively and this is not practically possible.

In the high cycle fatigue regime defects are more prone to cause the final failure while at higher load ranges final fracture can have its origin both from defects and microstructural weaknesses (i.e. grains or grain boundaries in an unfavourable direction). The propagation or nucleation of a crack requires a certain minimum energy and the smaller the load range the fewer defects or microstructural defects are activated. This is also why nucleation sites are more often sub-surface during HCF loading. In recent years there has been an increasing interest for ultra high cycle fatigue and lives up to 10^9 cycles. Testing is then made at very high frequencies that may cause problems with unwanted heating of the specimens and triggering of new mechanisms. It has been found that in some cases the fatigue curve has a steeper slope in the ultra high cycle fatigue regime than found during conventional HCF testing. Also the failure location is more often inside the specimen volume rather than at the surface.

4.1 High Cycle Fatigue Testing

HCF testing is usually carried out in load control using specimens with hour-glass shape or parallel gauge section (smooth or notched). The requirements for alignment, temperature distribution and load measurements are the same as for LCF tests (see Section 3.1). There are a number of ways to carry out HCF testing. One approach is to perform the tests primarily at load ranges where the specimens are expected to fail in a life range from approximately 100 000 cycles and up to 10^7 cycles. In this case a Basquin type of curve may be obtained:

$$\Delta\sigma = \frac{A}{E} \cdot N_f^\alpha \quad \text{or} \quad \log \Delta\sigma = \log \frac{A}{E} + \alpha \cdot \log N_f \quad (12)$$

Using this curve the fatigue limit can be obtained (extrapolation is usually necessary).

A second approach is to only aim for the fatigue limit and perform testing as close to the real fatigue limit as possible. In case a specimen fractures before 10^7 cycles the stress range is decreased by a small amount and for the coming specimens the stress range is decreased until a specimen survives 10^7 cycles. If a specimen survives 10^7 cycles the stress range is increased by a small amount and for the coming specimens the stress range is increased until failure occurs within 10^7 cycles. Using these simple rules the fatigue limit can be accurately determined if the probability of failure is plotted as a function of the stress levels used.

Of course, it is favourable to use a combination of the two approaches. This gives the Basquin-equation and an accurate determination of the fatigue limit.

4.2 High Cycle Fatigue – Effect of Mean Stress

The fatigue life in HCF is quite sensitive to the mean stress. There are a number of ways to quantify the mean stress effect, and one way is to use a so-called Haig or Goodman -diagrams. In this diagram iso-fatigue life curves are plotted in a mean stress-stress amplitude diagram as is shown in Figure 14-9. Any fatigue life may be plotted in the Haig diagram. For design purposes the Haig diagram is often truncated by the yield stress as is shown in Figure 14-9.

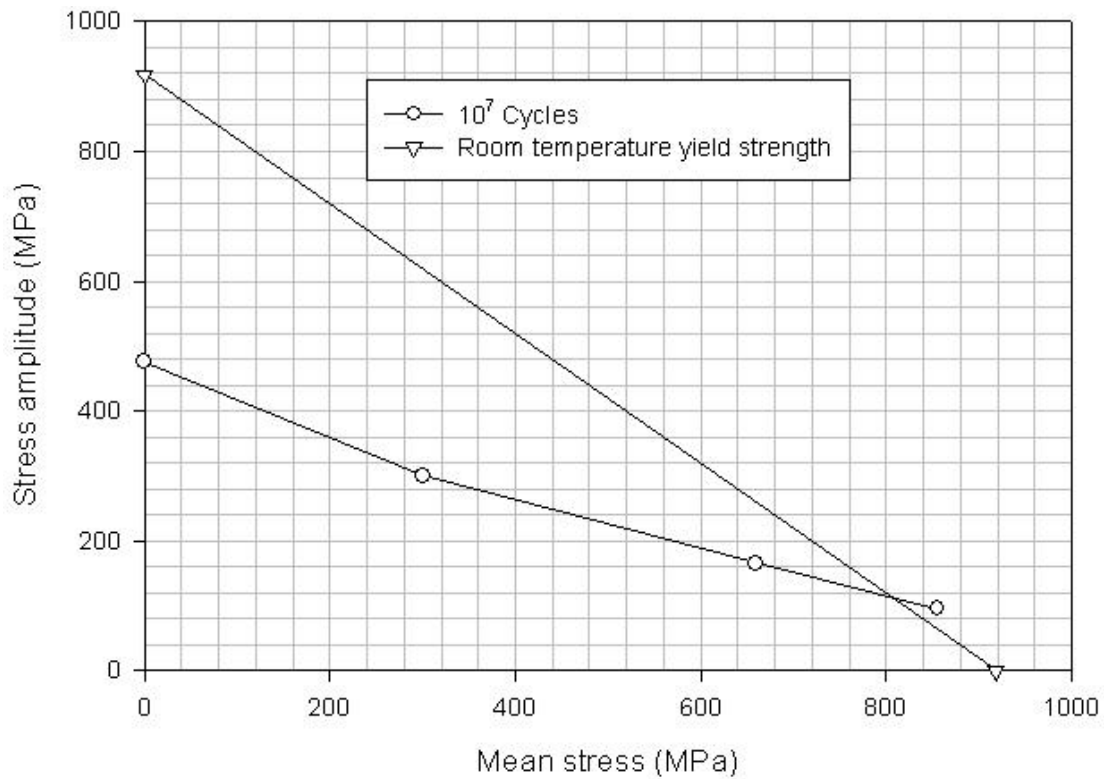


Figure 14-9: Haig diagram for a Ti –alloy at room temperature.

5.0 CRACK PROPAGATION

Crack propagation will always take place when components fail under fatigue conditions, both during LCF and HCF loading. In front of the crack tip the load situation can schematically be described as in Figure 14-10. As can be seen in Figure 14-10 the cyclic plastic zone is significantly smaller than the monotonic plastic zone in front of the crack tip.

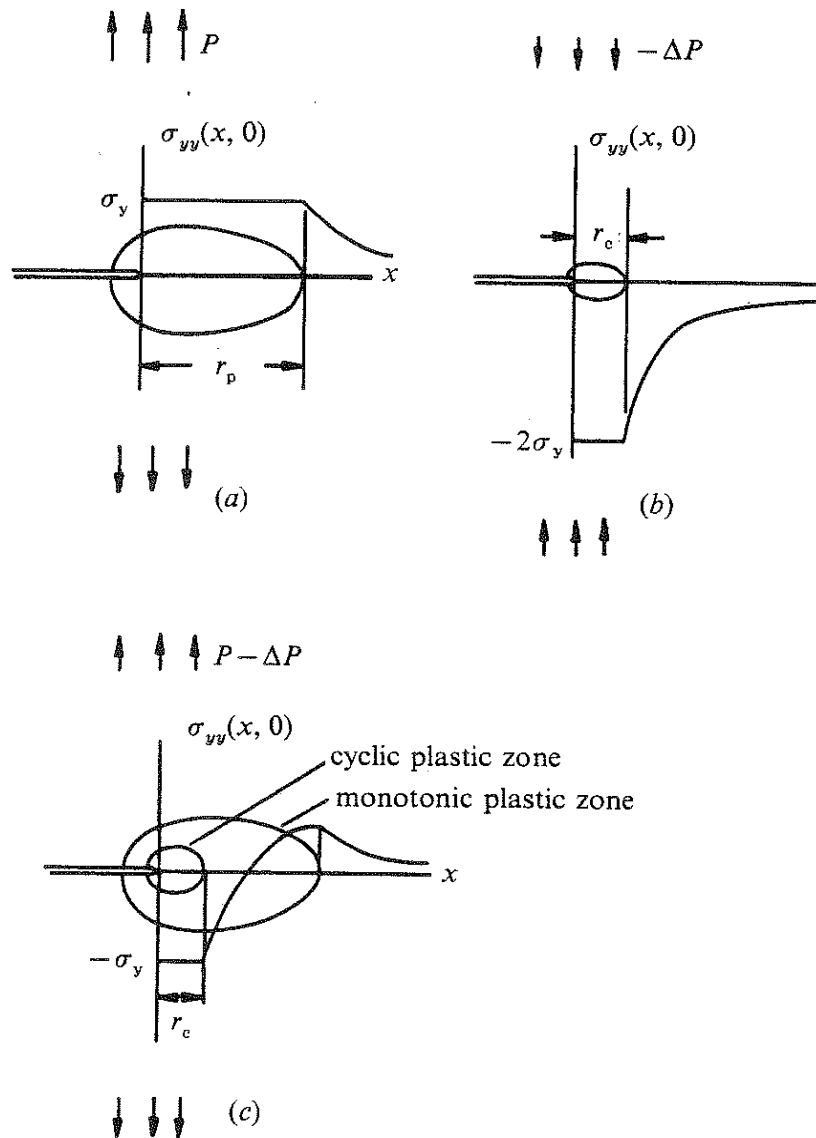


Figure 14-10: Schematic showing the stress distribution and plastic zone size during (a) monotonic loading to load P , (b) stress distribution due to unloading by ΔP and (c) superposition of the two load cases (a) and (b) [8].

Usually fatigue crack growth is treated using Linear Elastic Fracture Mechanics (LEFM). The fatigue crack growth rate under LEFM is often described by the Paris Law:

$$\frac{da}{dN} = C \cdot \Delta K^n \tag{13}$$

where da/dN is the crack growth per cycle, C and n are a constant and an exponent to fit with materials data and ΔK is the stress intensity factor range defined as:

$$\Delta K = Y \cdot \Delta \sigma \cdot \sqrt{\pi \cdot a} \tag{14}$$

Where Y is a geometry factor, $\Delta \sigma$ is the stress range and a is the crack size. The geometry factor for a number of common standard geometries and load distributions may for example be found in [9].

The logarithmic version of Equation 13 represents a straight line in the da/dN vs. ΔK diagram which makes the determination of the constant C and the exponent n easy.

If the load range is small (HCF-loading), the plastic zone size is small and the crack growth behaviour can be treated using linear elastic fracture mechanics. If the plastic zone size in front of the crack tip is large linear fracture mechanics is not applicable and crack growth has to be described in terms of ΔJ [8] or by the strain energy factor range ΔK_ε [10] (see Equation 15).

$$\Delta K_\varepsilon = Y \cdot \Delta \varepsilon \cdot E \cdot \sqrt{\pi \cdot a} \quad (15)$$

Where $\Delta \varepsilon$ is the strain range, E is Young's modulus and n is the crack growth exponent.

If a component is subjected to LCF loading crack propagation will occur practically from the first cycle and short crack growth needs to be taken into account. As is shown in Figure 14-11 the short crack growth behaviour is different from that for longer cracks. The reason for the large scatter in crack growth rate for short cracks is that crack growth is very fast (usually stage I crack) until a microstructural barrier is encountered which cause retardation of the crack until the barrier is overcome. One way to avoid the difficult short crack regime is to assume that the crack of a certain size is already present from the beginning. This is not always a bad assumption since the crack growth for small cracks is usually much higher than for long cracks. During LCF loads the conditions for linear elastic fracture mechanics will normally not be fulfilled and the crack growth needs to be quantified using the J-integral or more simple by using the stress range from a linear elastic calculation rather than an elasto-plastic calculation. The use of linear elastic stresses was suggested by [10] as a modification of the Paris law as:

$$\frac{da}{dN} = C \cdot \Delta K_\varepsilon^n \quad (16)$$

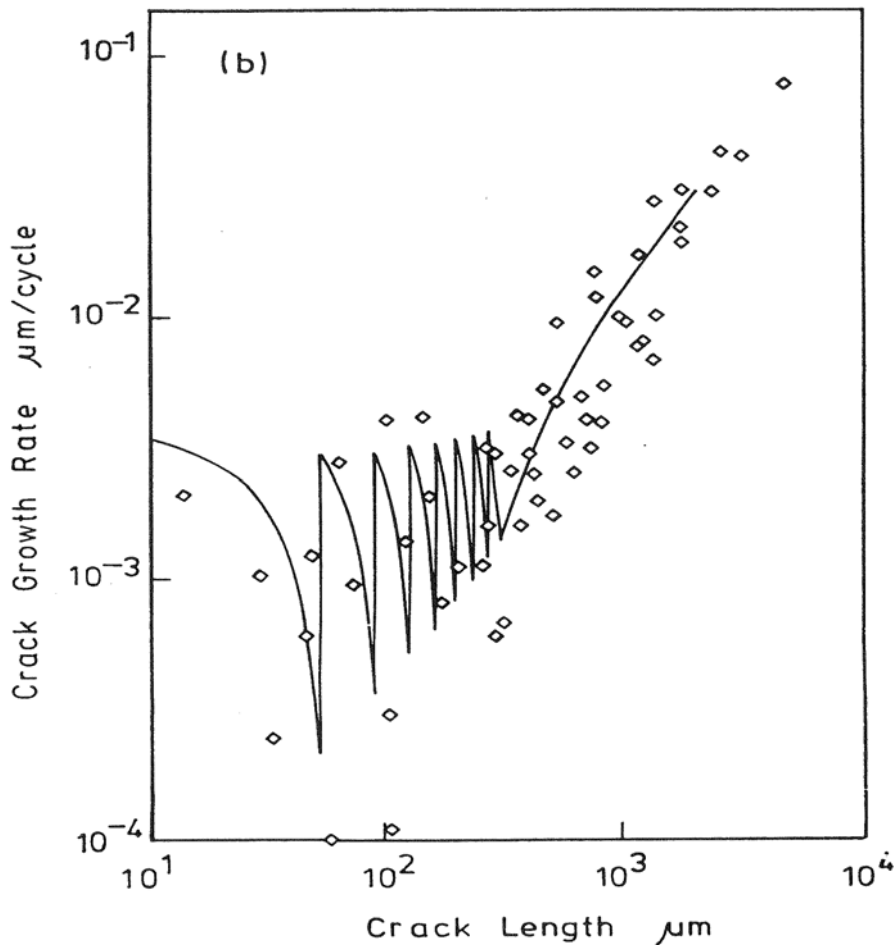


Figure 14-11: Schematic showing the transition from the short crack growth behaviour to the long crack growth behaviour.

A component subjected to HCF loads will in general not see any crack growth at all if the stress intensity factor is below the threshold value for crack growth, ΔK_{th} .

For HCF loads it is of less importance to worry about small crack growth since the crack size required to exceed ΔK_{th} is in most cases larger than the crack size where small crack growth is applicable (even if LEFM conditions according to ASTM E647 or 740 are not entirely fulfilled).

5.1 Crack Propagation Testing

For most gas turbine applications (and aircraft engines in particular) low weight is essential and consequently the load experienced by different components is very often high. A high load does not allow long cracks and therefore crack propagation testing is often made using specimens with relatively small semicircular surface or corner cracks rather than the more conventional through thickness cracks on Compact Tension (CT) specimens. Furthermore, crack propagation of surface or corner cracks is usually faster compared to through thickness cracks due to smaller amount of crack closure for the surface and corner cracks. The reason is mainly the constraint conditions at the crack front.

At Volvo Aero Corporation specimens with semicircular surface cracks are normally used for the crack propagation tests. Since the compliance change with crack growth is too small the crack extension is monitored using potential drop measurements.

A typical test set-up is shown in Figure 14-12. A starter notch approximately 0.075 mm deep, 0.150 mm long and 0.075 mm wide is Electro Discharge Machined (EDM) on the surface of one side. Notches are made larger for materials with large grain sizes in order to avoid failure at the wrong location. Thin wires of the same base material as the specimen are spot-welded on each side of the starter notch and on the opposite side two wires are spot-welded in order to have a reference signal for temperature compensation. During testing a constant DC current of about 10A is led through the specimen and the potential drop values over the crack and the reference wires, the applied load, and strain (if applicable) is measured at the maximum and minimum load during the fatigue cycle. When the crack is about 2 mm the bending stresses caused by the crack becomes significant and therefore the test is interrupted. In the normal case the specimen is then fractured at temperature to get a rough estimate of the fracture toughness.

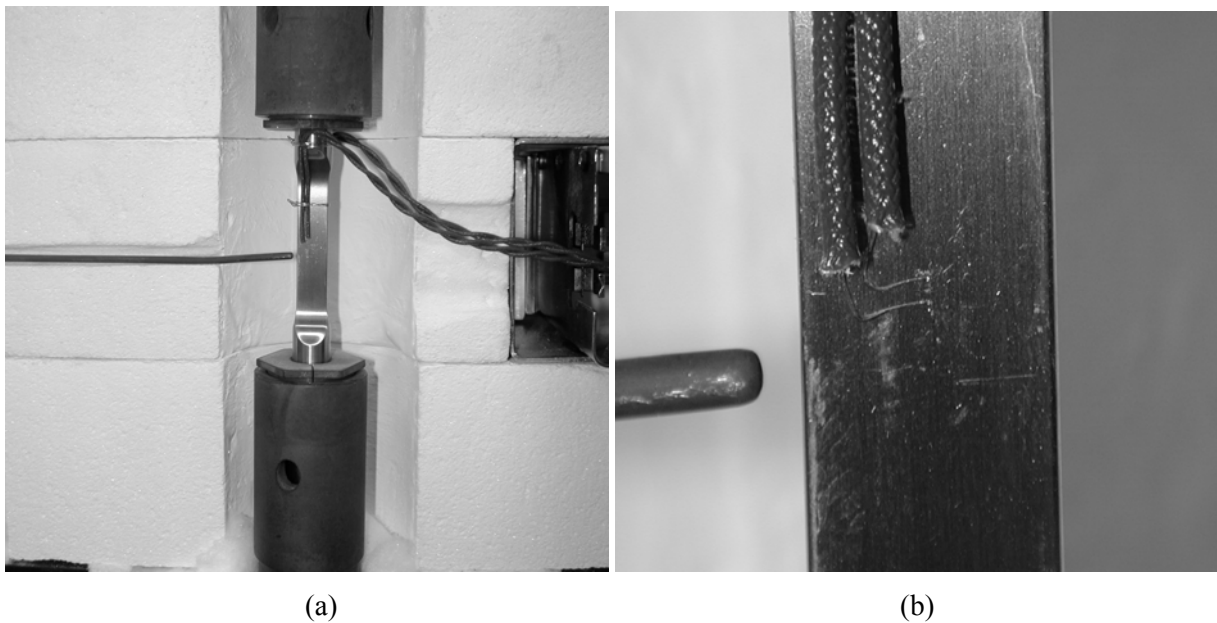


**Figure 14-12: Example of test set-up for elevated temperature crack propagation testing using Potential Drop (PD) technique on specimens with semicircular surface cracks.
(a) Overview of test set-up and (b) close up of instrumentation around notch**

The potential drop signal measured over the crack is normalised and made practically temperature independent by dividing it with the reference signal. Translation from the normalised potential drop signal to crack length can either be made by using a calibration curve (see Figure 14-13b) or a calculation of the potential field in the specimen. At Volvo Aero Corporation calibration curves are used. These may be obtained by marking the crack front at various potential drop values and fitting the obtained data to an equation. Markings may be made using heat tinting or overloads during short periods.

When the a vs. N curve is obtained the da/dN vs. ΔK may be calculated. It is important to avoid scatter in the data by using a large enough crack extension between two points used for calculating the da/dN value. Figure 14-13 shows how data is converted from potential drop values measured during a test to a da/dN - ΔK curve.

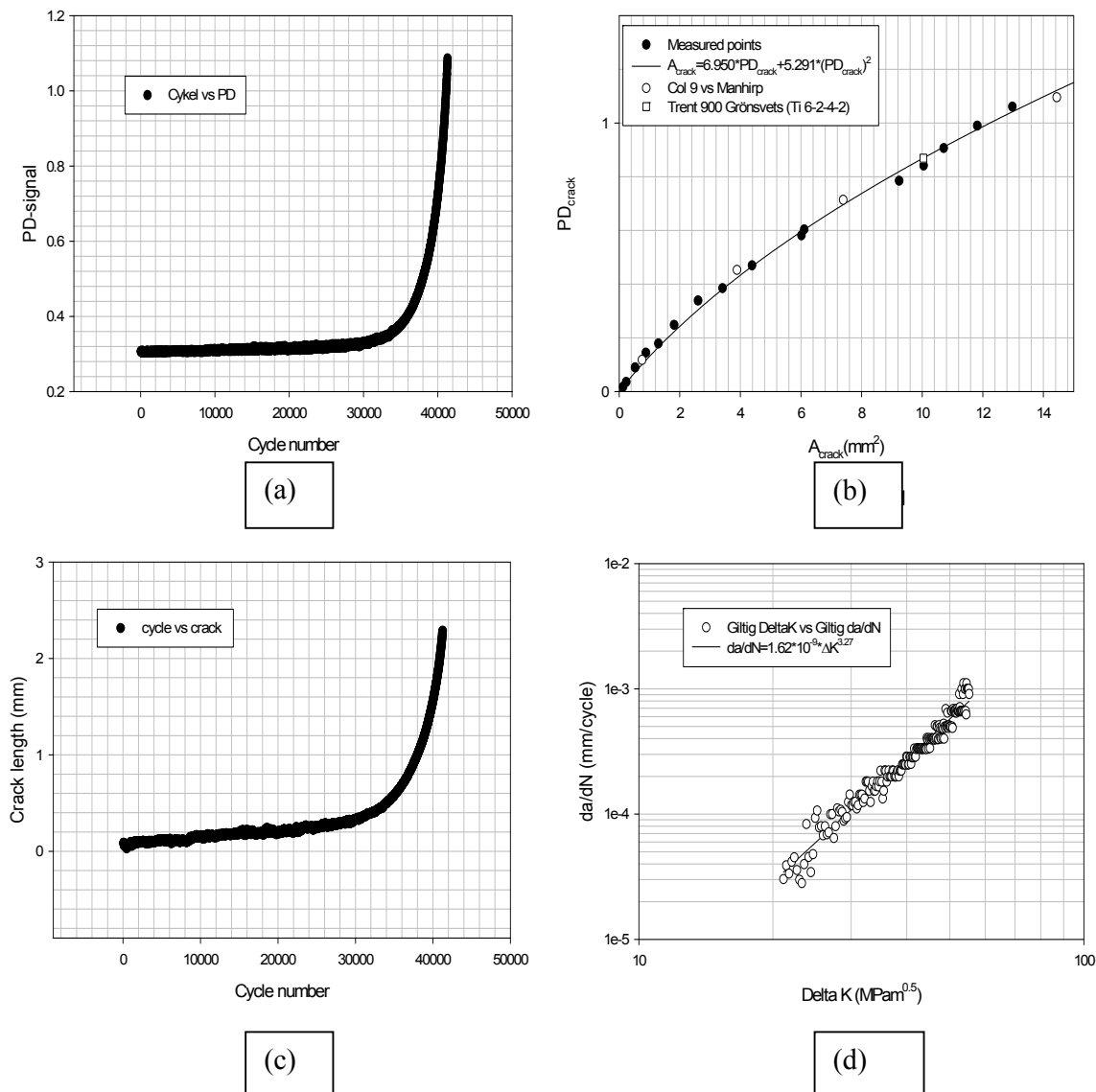


Figure 14-13: Example of how the measured potential drop values are converted to a $da/dN - \Delta K$ curve. (a) Potential drop value as a function of cycle number, (b) calibration curve, (c) crack length as a function of cycle number and (d) da/dN vs. ΔK curve.

In a similar fashion strain controlled crack propagation data may be generated. In order to generate conservative test results the extensometer for measuring the strain is placed on the opposite side of the specimen relative to the crack. Also for the strain controlled tests the tests are interrupted when the crack size is just above 2 mm. Instead of creating a da/dN vs. ΔK curve a da/dN vs. ΔK_{ϵ} is then created.

With decreasing ΔK the crack propagation rate decreases and the threshold value for crack growth, ΔK_{th} , under which crack growth does not occur or is very slow is usually defined as the ΔK when the crack growth is 10^{-10} m/cycle. This value is less than one broken atom layer per fatigue cycle. The ΔK_{th} value can be measured by decreasing the load in steps until the crack growth stops or by starting at a ΔK lower than the expected and then increase the load in steps until crack growth is detected in a specified number of cycles (usually about 10^6 cycles are needed) to ensure that the ΔK_{th} can be detected. ASTM recommends ΔK - decreasing method, but this is difficult to perform on surface crack specimens with a limited distance for crack growth available. At Volvo Aero Corporation ΔK_{th} is determined using the ΔK - increasing method after applying a number of compressive cycles to avoid residual compressive stresses in front of

the crack tip caused by the previous loads used to create the starter crack. The compressive load cycles create residual tensile stresses in front of the crack tip which suggests that the ΔK increasing method will give slightly too low threshold values. When using the ΔK - decreasing method there will always be an overload giving compressive loads in front of the crack tip which will always give an un-conservative estimate of the threshold value even if the maximum load decrease and the crack extension during each step is prescribed. Furthermore, when using the surface crack specimens the amount of crack extension is limited and consequently the number of load decreasing steps (with minimum crack extension in each step) is limited before the test becomes invalid due to bending. Figure 14-14 shows an example of threshold testing together with standard crack propagation tests.

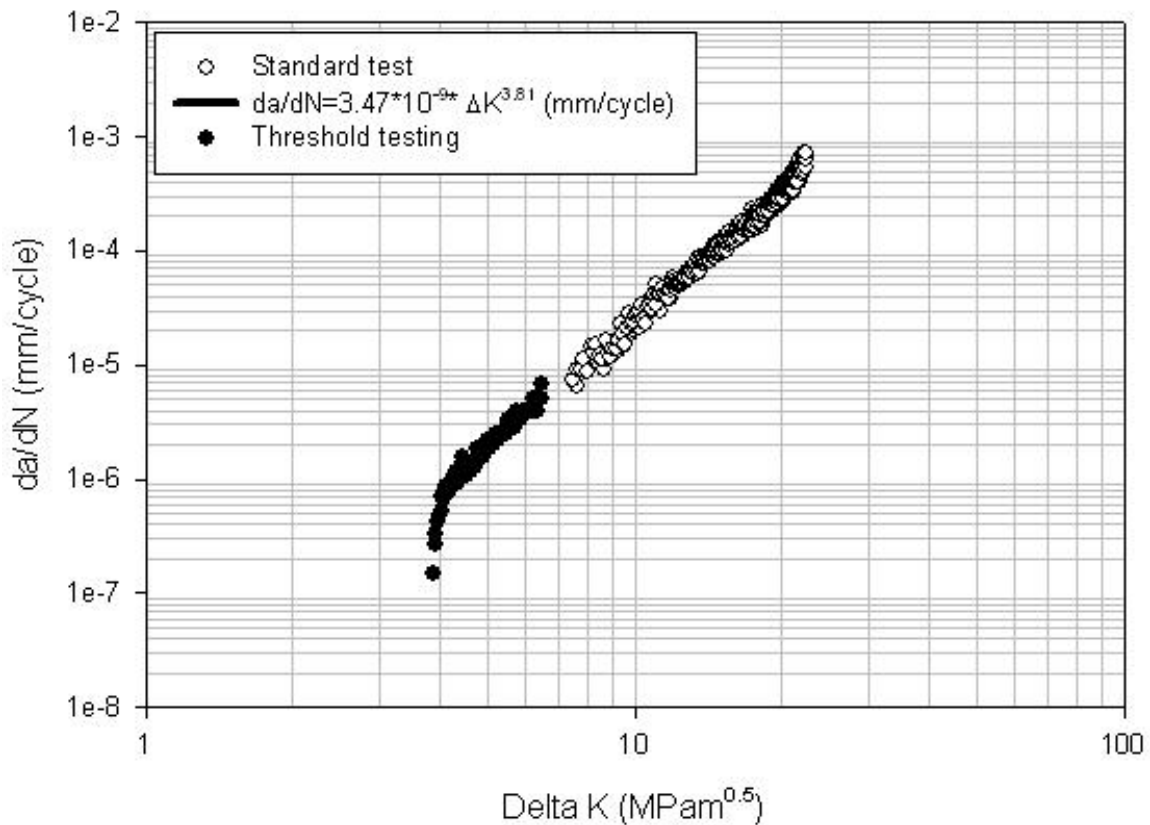


Figure 14-14: Example of crack propagation curve derived from 3 specimens, two in the Paris regime and one in the threshold regime.

5.2 Mean Stress Effect

Also in crack propagation there is an effect of the R-ratio on the crack propagation rate. The effect may be explained in terms of crack closure for R-ratios when the crack is likely to be closed during a significant part of the fatigue cycle. The part of the load cycle when the crack is fully closed does not contribute to the effective stress intensity factor range unless the compressive load causes the crack to open at a lower stress intensity than when it was closed during the unloading cycle. At R-ratios when the crack is open the whole fatigue cycle the R-ratio effect is much smaller. This is clearly illustrated in Figure 14-15 where iso- da/dN values are plotted in a $\Delta K - K_{max}$ diagram. At low R-ratios the effect of R-ratio is quite strong while at R-ratios above about 0.5 the effect is very small. The dominating factor for the R-ratio dependence at low R-ratios is most likely crack closure. One way to express the R-ratio dependence for crack growth is the Walker equation:

$$\frac{da}{dN} = C \cdot \frac{\Delta K^n}{(1-R)^R} \tag{17}$$

where C and n are Paris type constants and R is the Walker exponent.

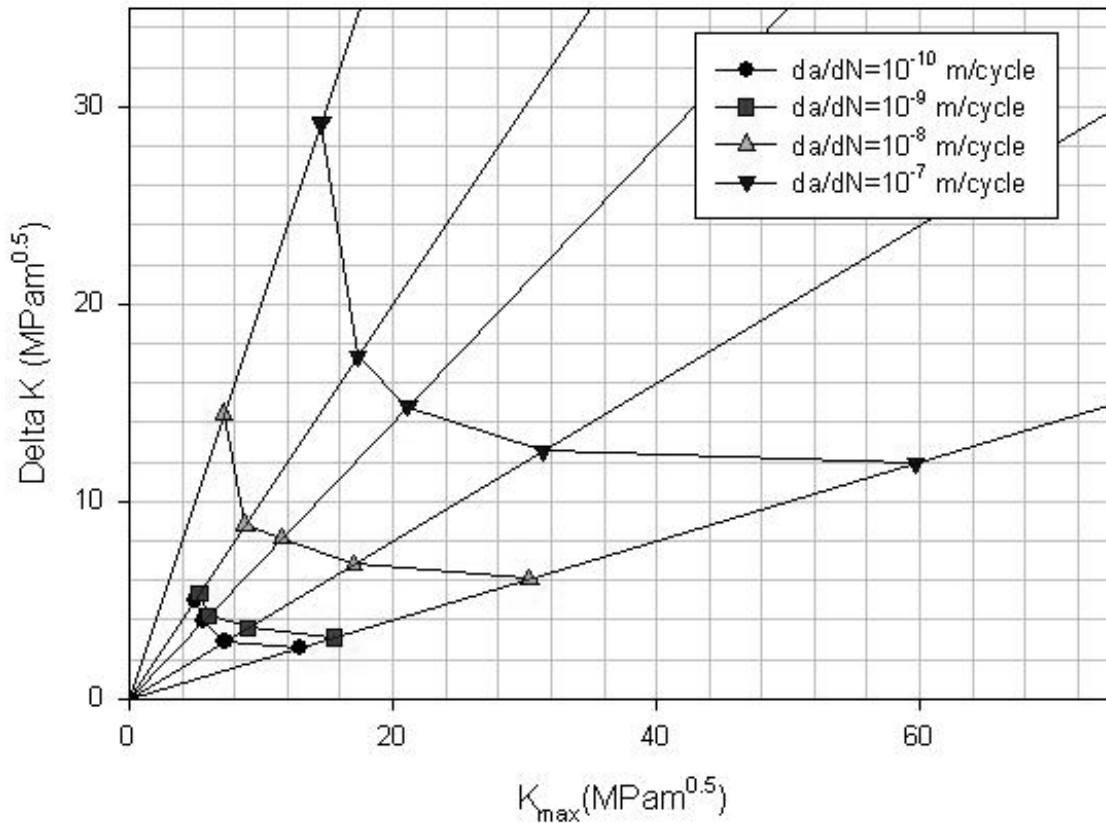


Figure 14-15.

5.3 Effect of Overload

The common understanding is that a single overload reduces crack propagation rate. This is believed to be the results of residual compressive stresses in front of the crack tip. However, it has been shown [11] that depending on the size of the overload and the stress intensity factor range both acceleration and retardation of the crack may occur.

5.4 Hold Time Effect on Crack Growth

The hold time effect on crack growth is quite complicated. An LCF cycle with hold times in compression and/or tension can be treated in terms of creep. For crack propagation however, there may be creep effects as well as degradation of the material, often the grain boundaries, in front of the crack tip. Experience has shown that both crack retardation as well as acceleration may occur. In the most severe cases reported, the crack growth curves with hold times up to 2h was shown to collapse completely when plotted in a da/dt vs. ΔK-diagram, where t is the time [12]. The sensitivity to hold time effects is material dependent and needs to be well understood to enable light weight and safe design.

6.0 LCF-HCF INTERACTION

The loading on components often consists of a combination of LCF loads (i.e. start-stop cycle) and small amplitude HCF loads (vibrations etc.). This problem may be treated as how the LCF loads influence on the HCF life or how the HCF loads influence on the LCF life. It is probably easier to understand the problem if the influence of the HCF loads on the LCF life is studied. It is unlikely that components intentionally are subjected to HCF loads above the fatigue limit. Consider a case with 10000 constant amplitude HCF cycles per LCF cycle. The damage accumulation for the HCF cycles in the beginning is zero since the HCF loads are below the fatigue limit. Damage accumulation from the LCF cycles starts from the very beginning and continues through out the life of the components. The damage accumulation from the LCF cycles finally creates a crack large enough for the HCF cycles to contribute to the damage or crack growth. When the crack size together with the HCF loading gives a ΔK above the threshold value for crack growth further damage is almost entirely caused by the HCF cycles. This is quite nicely illustrated in Figure 14-16. The contribution to the crack propagation from one LCF cycle compared to 10000 HCF cycles is below 1% even for ΔK close to the threshold value. The life of the component can therefore be considered over when the LCF loads have created a crack causing fatigue crack growth for the HCF cycles.

Ti 6-4, RT, CCF, R=0.8

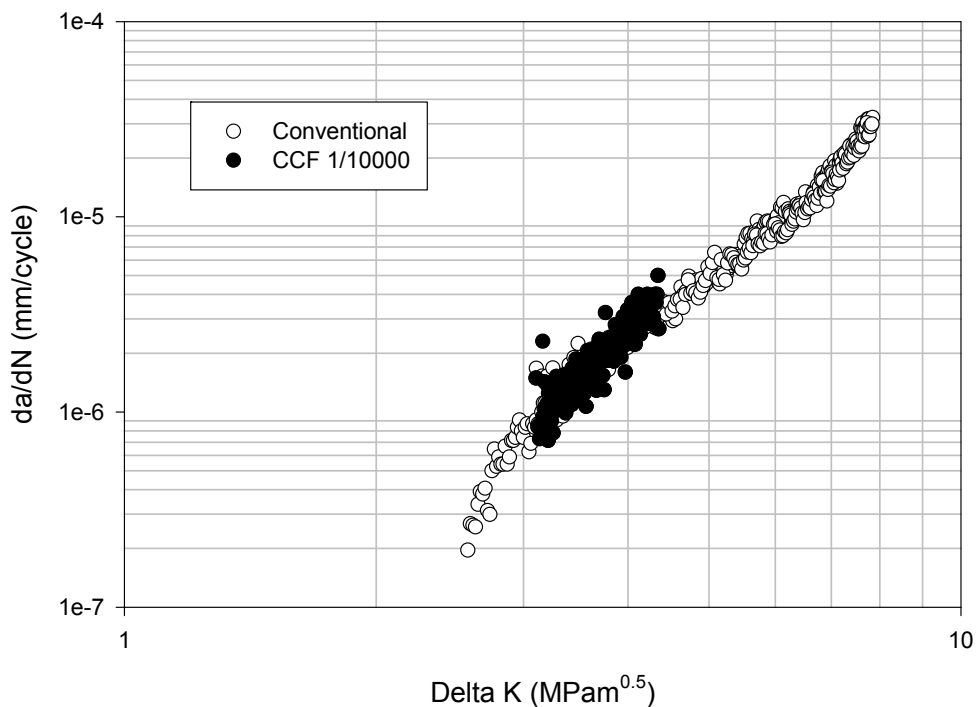


Figure 14-16: Crack propagation results for crack propagation tests at R = 0.8 and a test with 10000 HCF cycles per LCF cycle. The LCF cycle had R = 0 and same maximum stress as the HCF cycles.

7.0 REFERENCES

- [1] Albert, W. A. J. (1838) “Über Treibseile am Harz” *Archive für Mineralogie Geognosie Bergbau und Hüttenkunde*, vol. 10, pp 215-34.

- [2] Miller K. “Metal Fatigue- Past, Current and Future”, Proc. Instn. Mech. Engrs, vol 205, pp 291-304, 1991.
- [3] Ma, B. T. and Laird, C. , “Overview of Fatigue in Copper Single Crystals-II, Population, Size and Growth Kinetics of Stage I cracks for Tests at Constant Strain Amplitude. Acta Met. **37**, pp 337-48, 1989.
- [4] Basquin, O. H. “The Exponential Law of Endurance Tests”, Proceedings of the American Society for Testing and Materials,**10**, pp. 625-30, 1910.
- [5] Coffin, L. F. “A Study of the Effects of Cyclic Thermal Stresses on a Ductile Metal”, Trans. Am. Soc. of Mech. Eng., **76**, 931-50, 1954
- [6] Manson, S. S. “Behavior of Materials under Conditions of Thermal Stress”, National Advisory Commission on Aeronautics: Report 1170, Cleveland, Lewis Flight Propulsion Laboratory, 1954.
- [7] Natrella, M. G. , Experimental Statistics, National Bureau of Standards Handbook 91, Washington, USA, 1963.
- [8] Suresh, S. “Fatigue of Materials” , Cambridge University Press 1991.
- [9] Tada, H., Paris, P. and Irwin, G. R., The Stress Analysis of Cracks Handbook, 3 ed, The Am. Soc. Mech. Eng., New York, 2000.
- [10] Haigh, J. R. and Skelton, R. P. “A Strain Intensity Approach to High Temperature Fatigue Crack Growth and Failure”, Mater. Sci. Eng., 36, pp133-137, 1987.
- [11] Jacobsson, L. “Thermo-Mechanical Fatigue Crack Propagation in Inconel 718, Doctoral Thesis, Department of Mechanical Engineering, Materials Engineering, Lund University, 2007.
- [12] Telesman, J., Gabb, T. P., and Kantzos, P., Effect of Overloads on Time Dependent Fatigue Crack Growth in a Nickel Based Superalloy, pp. 2879-86, in Proc. Of the Eighth International Fatigue Congress, Stockholm, Sweden, 2002.

